Effects of Nitrogen and Carbon Dioxide Gases on the Degradation of Low-Density Polyethylene During Extrusion and Origin of the Color

C. Dubrocq,[1] M. Milesi,[1] G. Ramès-Langlade,[2] B. Monasse[1]

[1]*Centre de Mise en Forme des Matériaux, Ecole des Mines de Paris, UMR 7635, Rue Claude Daunesse BP 207-06904 Sophia Antipolis, France*
[2]*Air Liquide, Centre de Recherche Claude Delorme, Jouy-en-Josas, France*

Received 27 February 2007; accepted 1 June 2007
DOI 10.1002/app.27408
Published online 30 November 2007 in Wiley InterScience (www.interscience.wiley.com).

ABSTRACT: The effect of inert gases, nitrogen and carbon dioxide, on the oxidative degradation of low-density polyethylene appearing as colored spots has been studied during an extrusion process in competition with an antioxidant. Extrusion under inert gases significantly decreases the degradation level in the critical region of the process in comparison with classical extrusion under air. The effect of antioxidants on degradation during extrusion at a high temperature is weak. The main processes acting on this reduction of polymer oxidation and the origin of the color of degraded domains have been investigated. Energy-dispersive spectra of particles have confirmed that degradation is caused by thermooxidation. The nature of chromophore groups in degraded areas has been identified by IR microscopy. We found that β-conjugated ketoenols are present inside colored spots and seem to be responsible for the color of degraded parts. Quantum calculations have confirmed that such chemical structures absorb visible light and create reddish and brown colors. © 2007 Wiley Periodicals, Inc. J Appl Polym Sci 107: 3373–3385, 2008

Key words: antioxidants; degradation; extrusion; polyethylene (PE); thermal properties

INTRODUCTION

Polymer extrusion is a continuous process used to obtain tubes, sheets, fibers, and films with a regularity of properties during the entire process. It can be applied to almost all thermoplastic polymers, with a major development of polyolefins such as polyethylene and polypropylene. This industrial process is interrupted when a defect in quality appears online or with a delay after an offline analysis. If the process goes on, more numerous, larger, and darker spots are released in the extruded material. The appearance of dark spots inside an extruded clear material leads to unacceptable parts that are rejected, and the process is stopped to solve the problem. It is known that dark spots are caused by polymer degradation, and consequently, some critical parts inside the extruder are cleaned to start production again.[1] This cleaning period is time-consuming and should be reduced as much as possible. This kind of defect is more obviously observed on thin transparent films, that is, in film-blowing or cast-film processes. This phenomenon is tremendous in transparent polymers such as polyethylene and especially low-density polyethylene (LDPE).

The polymer degradation of polyolefins under high-temperature extrusion (>220°C) is known to be mainly thermooxidative degradation.[2,3] An analysis of the O_2/N_2 ratio at the exit of extrusion has effectively showed that it is lower than in an air atmosphere, and this is explained by the oxidation of extruded polymer melts.[3] The importance of thermal oxidation is confirmed by IR analyses of degraded extrudates[4,5] and by gas chromatography of volatile products from extrudates.[6,7,20] Researchers have found aldehydes, ketones, and formic acid.

The polymer degradation is mostly initiated by an oxidative reaction rather than mechanical scission.[2,8] Holmström and Sörvik[9] also supposed that mechanical strains resulting from an extrusion process at very high temperatures (284–355°C) could be neglected in degradation reactions and be modeled by thermooxidation in a static mode. This hypothesis is consistent with an analysis of extrusion.[2,3] IR spectroscopy shows the development of carbonyl and *trans*-vinylene functions with conjugated forms in polymer melts. Holmström and Sörvik[10] thought that carbonyl and *trans*-vinylidene were responsible for the homogeneous coloration of the sample surface as an effect of low oxygen diffusion in the poly-

Correspondence to: C. Dubrocq (claire.dubrocq@ensmp.fr).
Contract grant sponsor: Air Liquide Co.

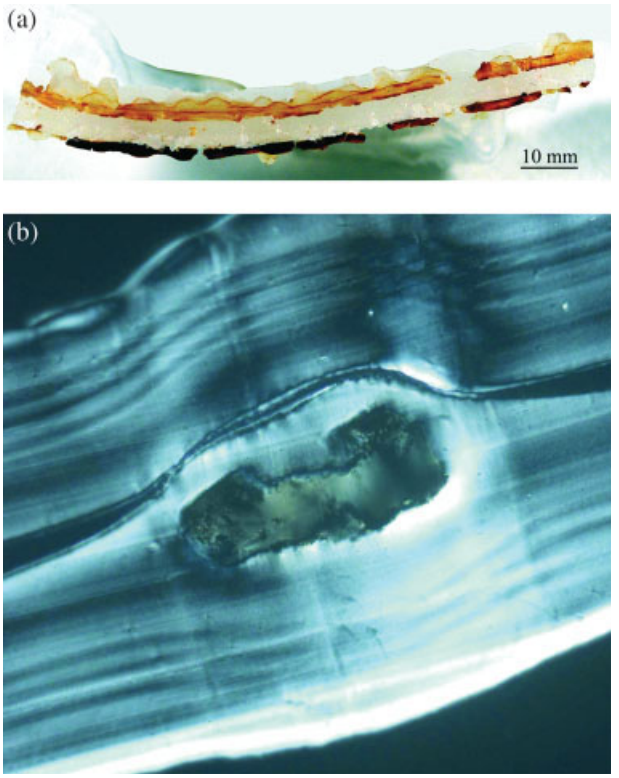

Figure 1 Degradation coming from the extrusion process: (a) degradation in stagnation areas of a split die (collected sample) and (b) 12-μm-thick cut of a sample in the final product containing a relaxed particle (observation under light polarization; dimensions: 335 μm × 260 μm). [Color figure can be viewed in the online issue, which is available at www.interscience.wiley.com.]

mer melt. However, the carbonyl groups do not produce any absorption in the visible optical range, and there is no associated chromophore.

Other studies[11] have suggested that phenolic antioxidants, often used as melt-processing stabilizers at high temperatures, can produce colored derivatives at the beginning of the visible degradation. However, numerous contradictions exist in the literature about color development due to stabilizer reactions. Thus, during extrusion, the degradation zones appear as spots and not as uniform degraded zones under static conditions. This difference of morphology should be connected to the dynamic conditions encountered by the polymer in the extrusion process but has not really been explained up to now.

A preliminary study was performed on an industrial LDPE removed from the inlet of a flat die after long-time extrusion in which spots appeared in the final product.[1] It showed a high concentration of spots with gradations of size and color from yellow to black [Fig. 1(a)]. Microscopy observations under polarized light of ultramicrotomed cuts in these corners showed a high number of colored spots concentrated along flow lines similar to recirculation flow lines[12] [Fig. 1(a)]. Outside these zones, the material was free of spots and seemed to be unshaded. Dark particles inside an industrial LDPE cast film were observed on a thin ultramicrotomed cut and were very similar to the individual dark spots observed inside the critical part of the die [Fig. 1(b)]. We think that this zone is critical for polymer degradation, and we have focused all our analyses on this zone.[13]

In this article, we compare the degradation after extrusion of polyethylenes under inerting gases (nitrogen and CO_2) and air. These gases are chemically stable according to their high enthalpy versus oxygen (Table I), and carbon dioxide is more soluble than nitrogen gas in polymers.[14,15] These conditions of degradation with inerting gases have been applied to two LDPEs, one free of antioxidant and the other one containing a classical formulation of antioxidants. This is one way to check the effects of an antioxidant and inerting gas. LDPE pellets have been extruded under the same conditions, and the material including spots has been systematically extracted from the inlet of a die after 8 h. The die has allowed the simulation of the stagnation area because of sharp contraction. The number and volume of colored spots collected in this stagnation zone have been measured by image analysis. This is a way to discuss the effects of the materials and processing parameters on degradation and to analyze how the gas is conveyed from the hopper to the die. Energy-dispersive spectrometry (EDS) under scanning electron microscopy (SEM) of dark spots has confirmed degradation in the polymer melts. IR analyses of individual spots with various colors have shown their chemical degradation and an experimental link between color and chemical degradation. Quantum mechanic simulations are able to predict the IR and ultraviolet–visible (UV–vis) spectra and to propose the chemical functions responsible for color. Finally, a mechanism is proposed for the formation of spots during the extrusion process.

TABLE I
Typical Bond Enthalpy

	Bond					
	C—H	C—C	C—O	O=O	C=O	N≡N
Bond enthalpy at 25°C (kJ/mol)	415	345	357	493	803	945

TABLE II
Physical Properties of LDPE

	LDPE without antioxidant 1003FE23 (Atofina)	LDPE with 1500 ppm antioxidant Lupolen 3721 C (Basell)
Melt index (g/10 mn)	0.3	0.1
Melt temperature (°C)	114	127
Density (g/cm^3)	0.923	0.937

EXPERIMENTAL

Materials

The two LDPE resins selected for this study were 1003FE23 (Atofina, Paris la Défense, France), without any antioxidant, and Lupolen 3721C (Basell, Hoofdoorp, The Netherlands), with antioxidants. 1003FE23 has few additives and no antioxidant, as proved by UV analyses of the initial material, whereas Lupolen 3721C contains 1500 ppm antioxidants (1000 ppm phosphites and 500 ppm phenol Irganox 1010). The main properties of these polymers are summarized in Table II. The antioxidant Irganox 1010 is known to produce during extrusion degradation derivatives such as chinones, which are chromatic groups.[16] These two LDPE resins are typically used for cast-film applications.

Extrusion equipment

All the experiments were performed with a Haake laboratory extruder. It was a single-screw extruder with a 50-mm-diameter screw [length/diameter (L/D) = 25]. A 5-dm^3 airtight pellet reservoir fixed at the extruder input was connected to a gas feeding system to inert the pellets in the hopper with a slight pressure ($\sim 10^3$ Pa; Fig. 2). An Oldham Ox 2000 oxygenometer gas detector was used to check the air tightness of the reservoir, and we did not notice any gas leak. The reservoir volume was sufficient for an extrusion run for 8 h at extrusion speeds of 1–64 rpm.

SEM

A Philips XL30 ESEM LaB6 scanning electron microscope was used under controlled pressure (0.5 mbar H_2O) to observe colored particles in polyethylene films. Images were acquired with a backscattering electron detector. Samples were analyzed with EDS to determine chemical elements present in the different regions.

IR spectroscopy

IR spectroscopy is the usual method to determine the nature of chemical groups of a material from the vibration modes of chemical bonds in the molecule. Because of the highly heterogeneous nature of degradation, an IR microscope was coupled with a Fourier transform infrared (FTIR) spectrophotometer, which allowed us to delimit analysis areas with 100-μm^2 windows.

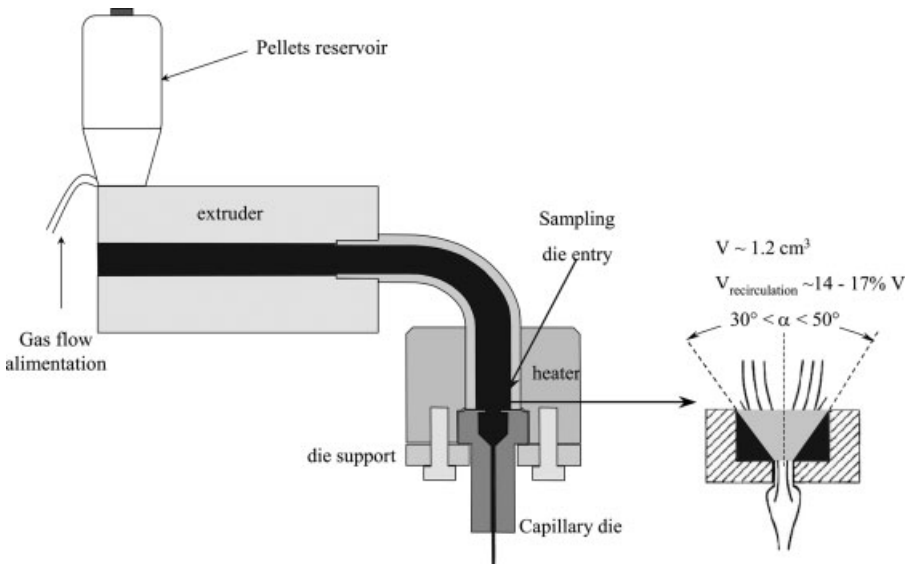

Figure 2 Capillary die system in line with extrusion.

TABLE III
Different Geometry of Capillary Dies

	Low-pressure die		Middle-pressure die	High-pressure die
L/D ratio	6.2	7.75	14.3	30
Length (mm)	6.2	6.2	10	30

An IR beam was focused with a Spectratech analytical microscope in the transmission mode (×15). The IR spectra were acquired on a Nicolet 510P FTIR spectrophotometer. One hundred twenty-eight scans at a 4-cm^{-1} resolution were coadded at a gain of 16 in the transmission mode.

Samples films were embedded in Nujol oil (aliphatic paraffin) between KBr plates to obtain local transmission spectra. The oil was used to avoid light scattering at the interfaces between the film and KBr plates and to remove the air layer. IR absorption curves between 1600 and 1800 cm^{-1} were fit to determine the peak wave numbers.

Experimental conditions

Processing conditions

Extrusions were performed for 8 h to simulate processing conditions under which degradation is usually observed. The same extrusion temperature was fixed at 270°C for all the experiments. It is a high temperature for processing polyethylene, which favors its thermal degradation, at the limit of its processing range.[1] Five temperatures were controlled for the processing conditions, four inside the extruder and one inside the die. The temperature profile was 120, 170, 220, and 270°C at the end of the extruder and in the capillary die. The temperature, measured with a thin K thermocouple (diameter ϕ = 250 μm), inside the die exit was 264 ± 3°C for 1003 FE23 and 267 ± 5°C for Lupolen 3721C. The atmosphere was controlled during the entire extrusion time in the hopper. A normal air atmosphere was maintained (78% N_2, 21% O_2, 0.9% Ar), or the atmosphere was inerted by a pure gas, N_2 (99.999%) or CO_2 (99.6%), which was regulated under a constant low flow rate (0.23 L/min) from Air Liquide bottles.

The other main adjustable parameters of this work are the extrusion rate and the die pressure. The flow rate depends on the screw speed and die pressure. The screw speed was fixed in the range of 1–64 rpm. As previously noticed, the critical zone for polymer degradation is located at the entry of the capillary die. A 6-mm-internal-diameter steel flat ring was located between the extruder head and the capillary die to increase the volume of degraded polymer in the stagnation zone (Fig. 2). Capillary dies with various L/D ratios were used to apply different die pressures at the same extrusion flow rate (Table III). In this way, it was possible, at the same flow rate, to decouple the effects of the screw speed (shear rate) and pressure on polymer degradation.

Experimental setup

Before each experiment, the extruder was purged for 30 min, and the die was cleaned of polymer with a blowtorch and then with acetone. For the experiment of inerting extrusion, a higher gas flow rate was applied previously to the extrusion experiment to remove most of the oxygen initially present in the extruder. Then, the gas flow rate was stabilized at a lower level during the entire extrusion process. After 8 h of extrusion under a controlled atmosphere, the samples were collected at the die entry and quenched in water to avoid any postoxidation. The collected volume was on average 1200 mm^3, and 15.5 ± 1.5% of the sample came from the stagnation zone (Fig. 2). To be independent of the collected quantity, all the data were normalized by the sample weight.

Then, polymer films 90 μm thick were prepared to favor the observation and analysis of degradation. The films were obtained by the pressing of each sample between hot plates backed by poly(ethylene terephthalate) films at 180°C under 200 bars for 5 min. During this step, we neglected the action of oxygen because the time of preparation was short in comparison to the 8 h of extrusion. The resulting films had a smooth surface necessary for observation and were easily removed from the poly(ethylene terephthalate) sandwich. Particular care was taken to repeat exactly the same conditions of pressure and time because it was a critical step for data analysis and comparison. All the samples were thus evaluated under the same extrusion conditions and also with the same procedure developed before. This provided a screening technique that allowed a direct comparison of samples within specified conditions.

Degradation quantification

LDPE films were scanned at an 8-bit depth for each color component in transmission at 1600 dpi with a white light. Such a resolution allowed us to catch degraded particles down to 250 μm^2. Images were

analyzed with Visilog 6.2 digital image analysis software. Degradation was detected from the mean gray level of the blue component of the scanned particles. Indeed, as the particles were rather reddish, it was the complementary color that allowed the best contrast in transmission. The gray level depends on the film transparency and the scanning system. As the samples were carefully prepared in the same way, the gray level of degradation detection was fixed and was equal to 180 when the white level was 255 and the black level was 0. The mean level through the undegraded sample was 70.

The degradation level was evaluated by two characteristic parameters obtained with Visilog 6.2: first, the number of degraded particles (mg^{-1}), and second, the total degraded area ($\mu m^2/mg$). The first parameter estimated the number of sites of degradation in the polymer melt, and the degraded volume was deduced from the second one. The particles smaller than the thickness (90 μm) were assumed to be spherical because degraded particles were harder than LDPE resins [Fig. 8 (shown later)] and seemed to be remain spherical after being pressed to obtain the films. The particles larger than the thickness should have been squeezed and fragmented during the film preparation, and we assumed that they were cylindrical in shape to approximate the exact geometry of particles observed under that condition. The total degraded volume (V_{ex}) was obtained by all the particles with these various shapes being counted:

$$V_{ex}(\mu m^3/mg) = \Sigma_{(\phi<90\ \mu m)} 4/3\pi R^3_{measured} + \Sigma_{(\phi>90\ \mu m)} \pi R^2_{measured} \times 90\ \mu m \quad (1)$$

where $R_{measured}$ is the radius of the degraded particle.

RESULTS AND DISCUSSION

Gas effects

Degradation appears as reddish, brown, or black particles (Fig. 3). Their size can vary from the resolution limit, 250 μm^2, to 0.6 mm^2. The particles smaller than 90 μm are spherical, whereas the bigger ones are more angular. The shape of the bigger particles might be caused by film preparation and particle squeezing. A strong reduction of the number of particles and their size has been observed after extrusion either under nitrogen or carbon dioxide from an air atmosphere at pressures ranging from 50 to 270 bars and screw speeds ranging from 1 to 64 rpm (Fig. 4). All the experimental conditions are summarized in Table IV. The number and mean size of the particles are significantly lower under an inert atmosphere: nearly 60% for LDPE 1003FE23 versus extrusion under air and 50% for LDPE Lupolen 3721C.

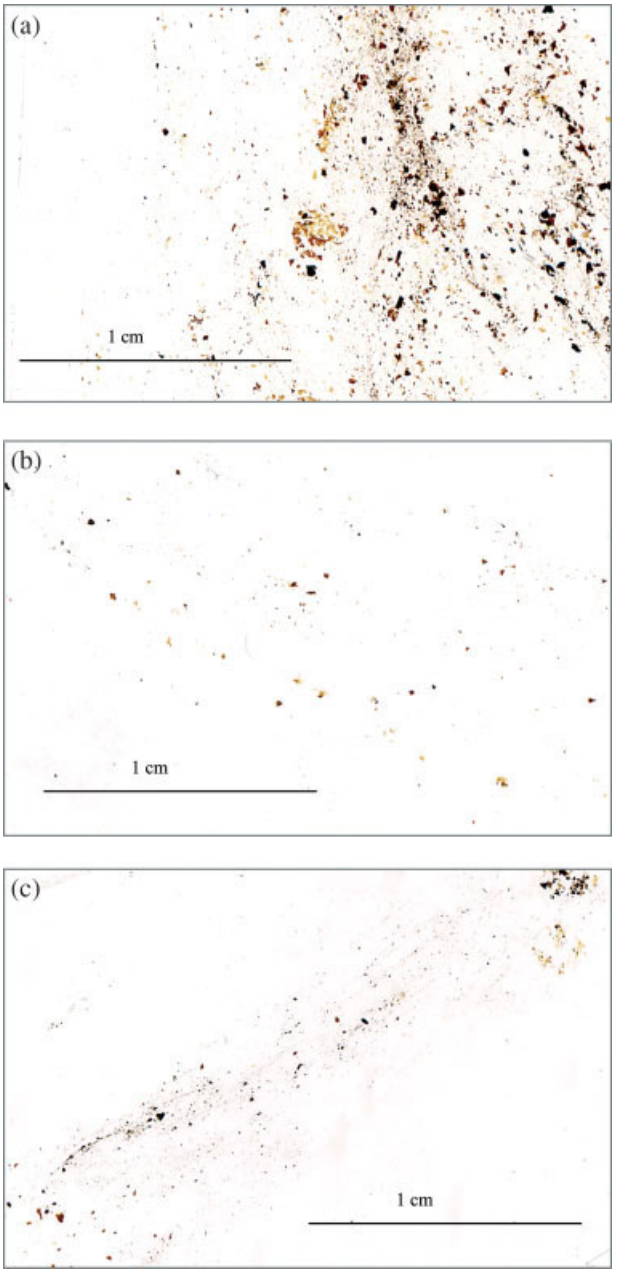

Figure 3 Films after extrusion in (a) air, (b) nitrogen, and (c) carbon dioxide. LDPE Lupolen 3721C was extruded at 16 rpm. [Color figure can be viewed in the online issue, which is available at www.interscience.wiley.com.]

As a result, it seems that the atmosphere in the feed hopper controls the degradation near the exit of the extruder. There is no direct connection between these two zones; the only way for the transit of gas is the molten polymer, and this implies gas dissolution in the polymer. Under static conditions, the dissolution of nitrogen and carbon dioxide gases in a molten polymer follows Henry's law: the solubility of a gas linearly increases with pressure.[17] Under

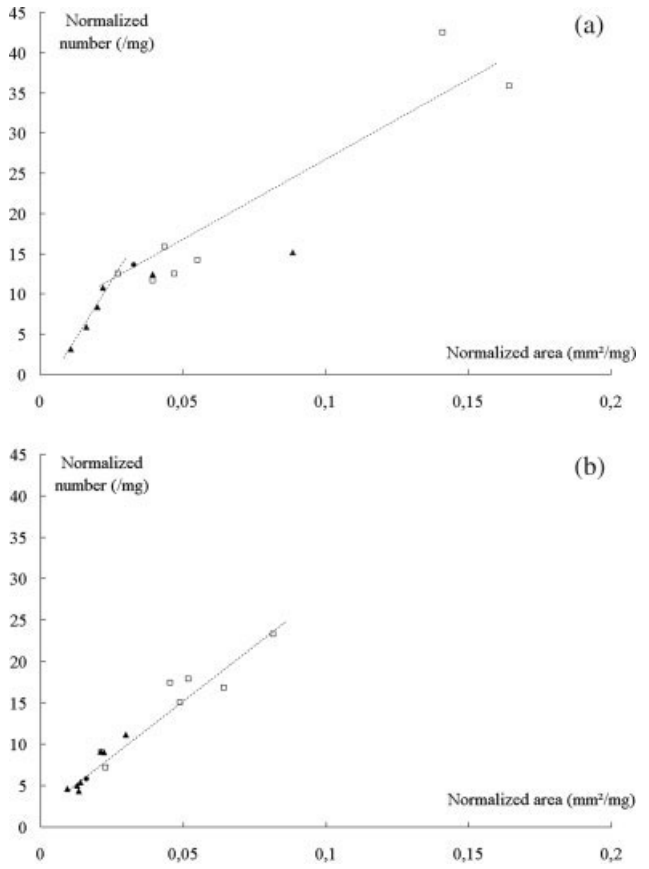

Figure 4 Number of degraded particles as a function of area in (□) air, (▲) nitrogen, and (●) carbon dioxide: (a) LDPE 1003FE23 and (b) LDPE Lupolen 3721C.

static conditions, the diffusion is the transport mechanism of gas. Under extrusion conditions, we expect convection to be the main mechanism of gas transport following the polymer melt. Then, it should be directly connected to the flow rate. It is difficult to predict the main factor that controls the gas content in the critical zone near the die entry: the gas solubility or its transport rate (Fig. 5). From 50 to 180 bars, degradation under air effectively increases with pressure, but above that, it drops. High pressure probably makes the relaxation of degraded particles in the extruded product easier. This is indeed the way of visualizing used by film manufacturers when production has to be stopped to clean the machine. We also observed a few dark spots in LDPE capillaries during extrusion, but it is very difficult to estimate the quantity of relaxed degradation in 8 h. In addition, degradation has been studied in terms of screw speed to check the effect of the shear rate on the mechanical degradation of polymer chains, which can promote thermomechanical oxidation (Fig. 6). The experiments have been carried out with two different capillary dies for both resins to confirm the trend and to decouple the effects of the shear rate and pressure on polymer degradation. There is

TABLE IV
Experimental Conditions of Extrusion

LDPE 1003FE23												
Screw speed (rpm)	64	1	8	16	64	8	16	45.2	64	16		
L/D ratio	6.2	7.75	7.75	7.75	7.75	14.3	14.3	14.3	14.3	30		
Pressure (bar)	102	50	105	125	167	135	183	224	270	200		
Tested atmosphere	Air, nitrogen	Air, nitrogen	Air, nitrogen	Air, nitrogen	Air, nitrogen	Air, nitrogen	Air, nitrogen, CO_2	Air, nitrogen	Air, nitrogen	Air, nitrogen		
LDPE Lupolen 3721C												
Screw speed (rpm)	8	16	64	8	16	45.2	64					
L/D ratio	6.2	6.2	6.2	7.75	7.75	7.75	7.75					
Pressure (bar)	108	128	183	190	205	252	280					
Tested atmosphere	Air, nitrogen	Air, nitrogen	Air, nitrogen	Air, nitrogen	Air, nitrogen	Air, nitrogen	Air, nitrogen					

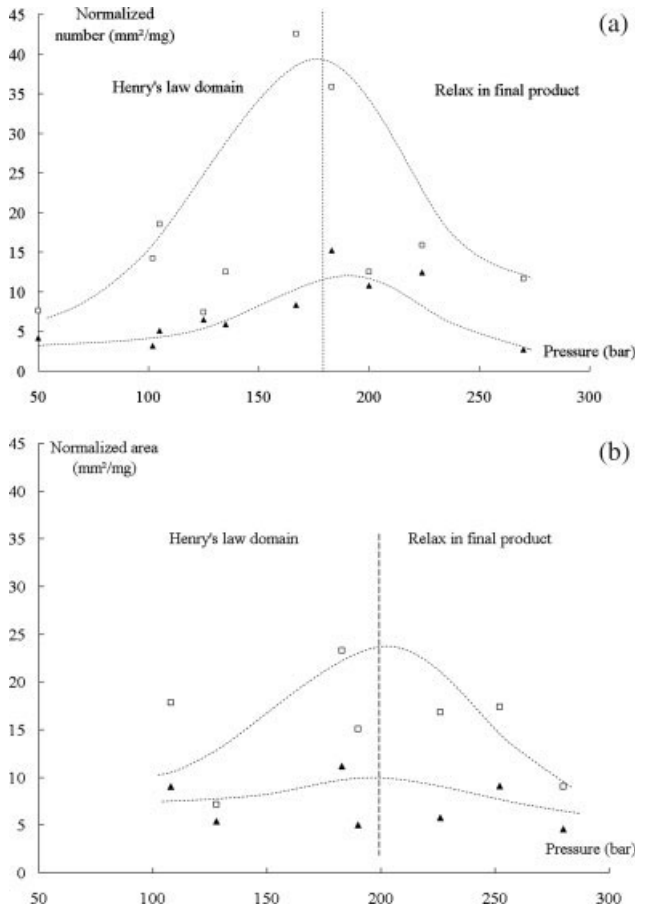

Figure 5 Effect of pressure on degradation in (□) air and (▲) nitrogen: (a) LDPE 1003FE23 and (b) LDPE Lupolen 3721C.

no relationship between the degradation quantity with screw speed and therefore to the shear effect. As a result, mechanical shear has little effect on degradation, and this confirms that the degradation is mainly thermooxidative rather than thermomechanical and oxidative.

Antioxidant effects

Contradictions in the literature about the role of antioxidants have led us to compare the degradation of 1003FE23 without any antioxidant and Lupolen 3721C containing an important quantity of antioxidants. Degradation of both LDPE resins is nearly the same as measured by the number of sites or volume of degradation, except for two experiments with unstabilized LDPE in air (Fig. 4). Let us further examine extrusion in air. It seems that the degradation of unstabilized LDPE is a little bit higher than that of LDPE with antioxidants. Therefore, it follows that antioxidants, especially Irganox 1010, are not responsible for discoloration. On the contrary, they very slightly prevent degradation for a long extrusion period but less efficiently than inerting.

Chemical nature of degradation

Colored particles coming from polymer melts have been analyzed with SEM (Fig. 7). Some visible areas of the particles on the optical picture were not seen in the electronic image because of a thin layer of polyethylene that covered part of the particles, but smaller regions have been individually analyzed. As expected, the pure polyethylene EDS spectrum reveals carbon and oxygen peaks. Oxygen detection in the pure resin is only due to the presence of water in the enclosure. The EDS spectra of the particles and polyethylene matrix are the same, but the oxygen peak is significantly higher in the particles (Fig. 8). In addition, the particles appear brighter than the polyethylene matrix, and this means that some heavier elements are present inside the particles. Therefore, we can conclude that particles contain a great atomic fraction of oxygen. Although EDS spectra can be only qualitative because of the presence of water in the analysis volume, the C/O ratio in particles

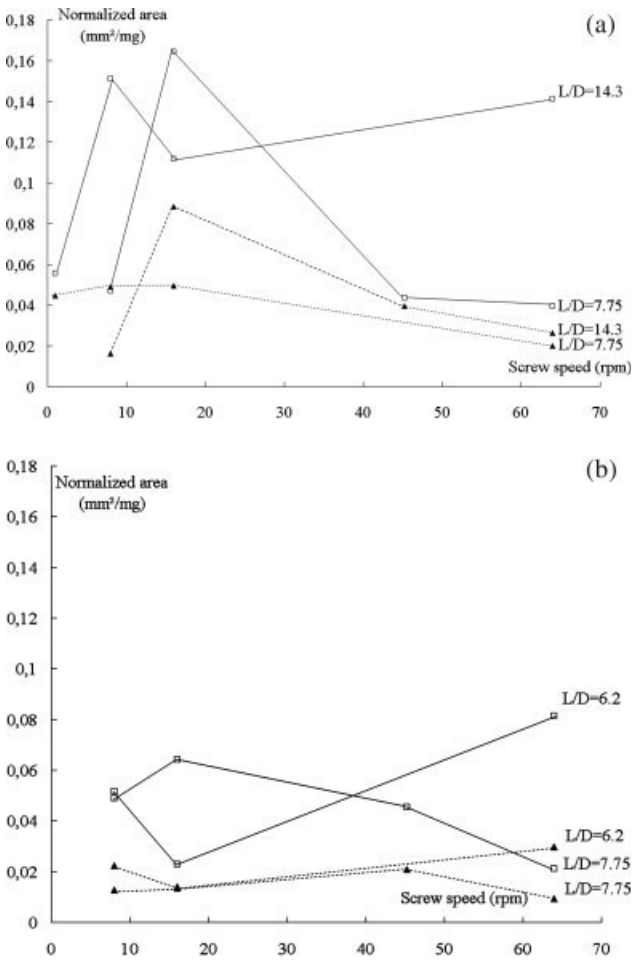

Figure 6 Effect of screw speed on degradation in (□) air and (▲) nitrogen: (a) LDPE 1003FE23 and (b) LDPE Lupolen 3721C.

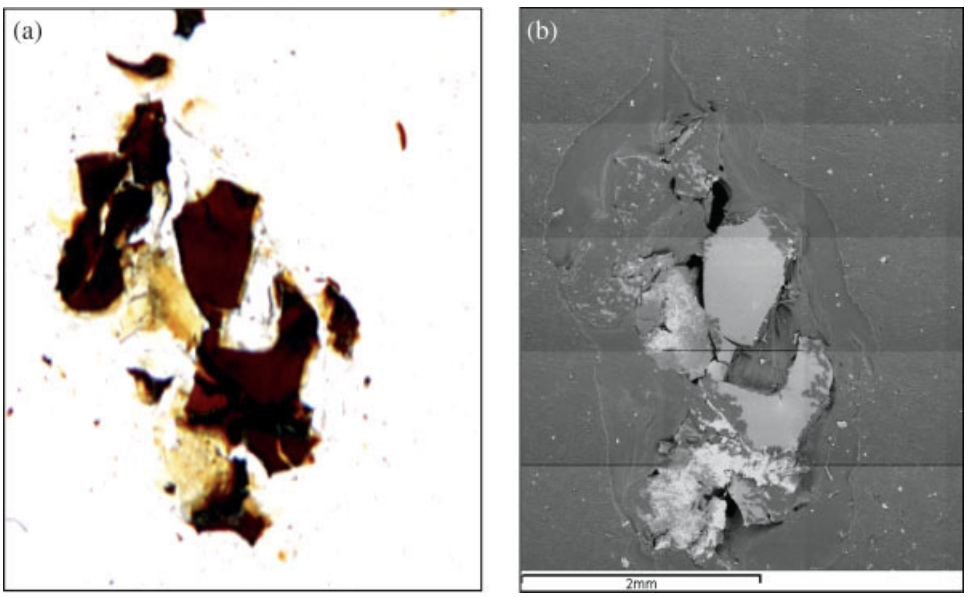

Figure 7 Brown particles in a polyethylene film: (a) optical and (b) SEM images. [Color figure can be viewed in the online issue, which is available at www.interscience.wiley.com.]

can be estimated if one assumes that detected oxygen coming from water vapor is nearly at the same level for the pure polymer and particles. According to this hypothesis, the C/O molar ratio in particles is equal to 2.77, that is, nearly 4 oxygen atoms for 11 carbon atoms. As a result, EDS gives evidence of a significant oxidation of degraded particles.

To confirm the action of oxygen on degradation, IR experiments have been performed on films obtained under all the extrusion conditions presented previously. Because of the size of the degraded particles, IR microscopy is a good means of evaluating IR spectra of degradation.

All the spectra of degraded particles acquired under different shear, pressure, and gas conditions are similar. Degradation has specific IR absorptions, especially between 3200 and 3700 cm^{-1}, which are caused by alcohol bonds, and between 1600 and 1800 cm^{-1}, which correspond to unsatured oxidized functions (Fig. 9). Other absorption bands are located at low wave numbers (950–1400 cm^{-1}) and are characteristic of a hydrocarbon backbone. Modification of hydrocarbon chains appears with oxidized functions. Consequently, degraded particles may come from polyethylene macromolecules that are degraded and oxidized.

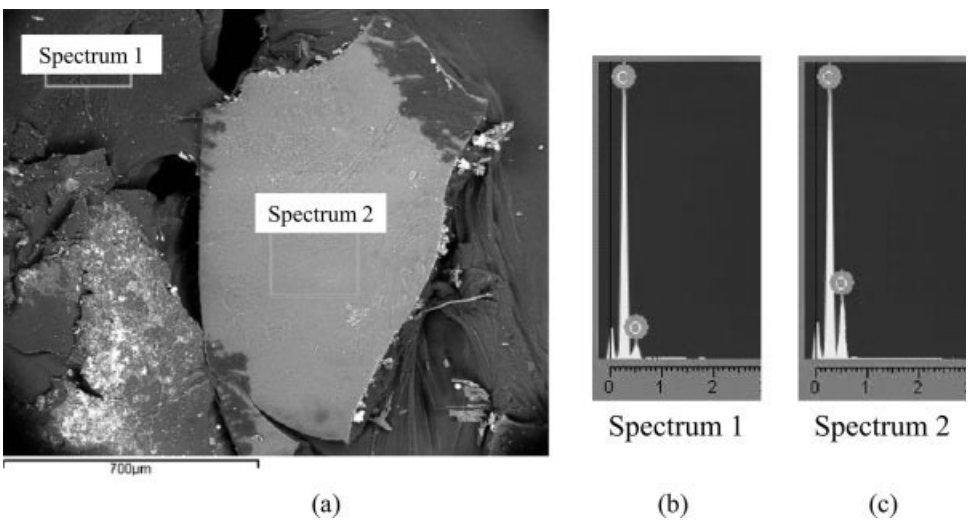

Figure 8 Polymer matrix and a brown particle with their respective EDS spectra: (a) areas analyzed by EDS, (b) pure LDPE, and (c) the brown particle (experimental conditions: L/D = 14.3, 16 rpm, 183 bars, under air).

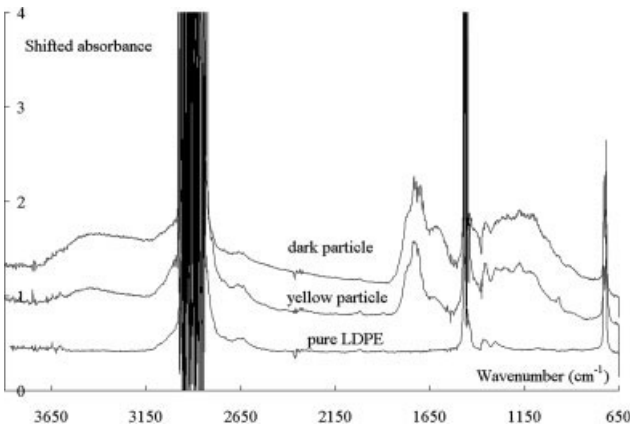

Figure 9 IR spectra of pure polyethylene and degraded particles from LDPE 1003FE23 (experimental conditions: L/D = 14.3, 16 rpm, 183 bars, under air).

Peaks between 1600 and 1800 cm^{-1} are fitted by a convoluted Lorentzian and Gaussian form:

$$I = \frac{I_0}{1 + \left(\frac{x - x_0}{2L}\right)^2 + \left(1 - \frac{cte}{2} e^{-\left(\frac{x - x_0}{2L}\right)^2}\right)} \quad (2)$$

where I_0 is the peak maximum intensity, x is the number of waves, x_0 is the peak number of waves, L is the peak width, and cte is a constant number.

According to the literature, the peaks are found with the following wave numbers: 1620, 1715, 1768, and 1740 cm^{-1} (Fig. 10). We faced this result with IR absorption tables that allowed finding the most suitable functions for comparing the relative intensity of each hypothetic function. We thus determined that the 1715-cm^{-1} peak is due to saturated aliphatic acids, 1740 cm^{-1} is due to saturated aliphatic aldehydes or esters, and 1620 and 1768 cm^{-1} are due to enol forms. The 1620-cm^{-1} peak is caused by vibration of a double carbon bond, whereas the 1768-cm^{-1} peak is caused by the ketone function. The enol form results from equilibrium with the ketone form. Acid, aldehyde, and ester functions do not absorb visible light in the optical range, whereas β-conjugated ketoenol, known to be a stable form of enol, can absorb visible light because of its conjugated double bonds.

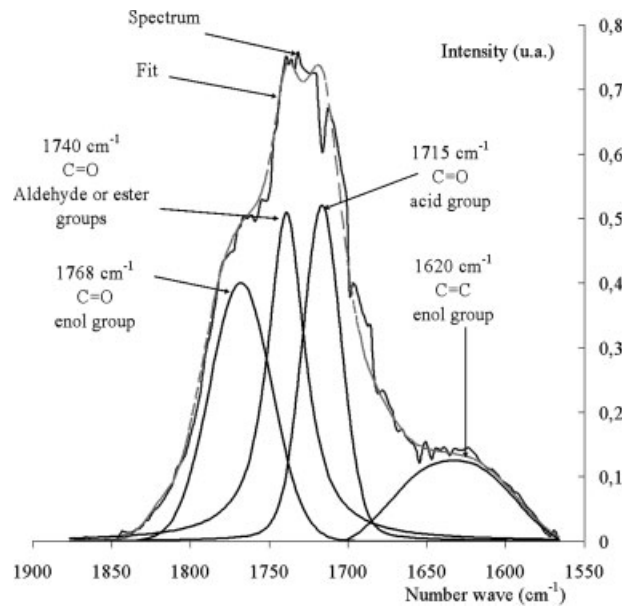

Figure 10 IR spectrum fitted from 1600 to 1800 cm^{-1} of a yellow degraded particle (experimental conditions: L/D = 14.3, 16 rpm, 183 bars, under air).

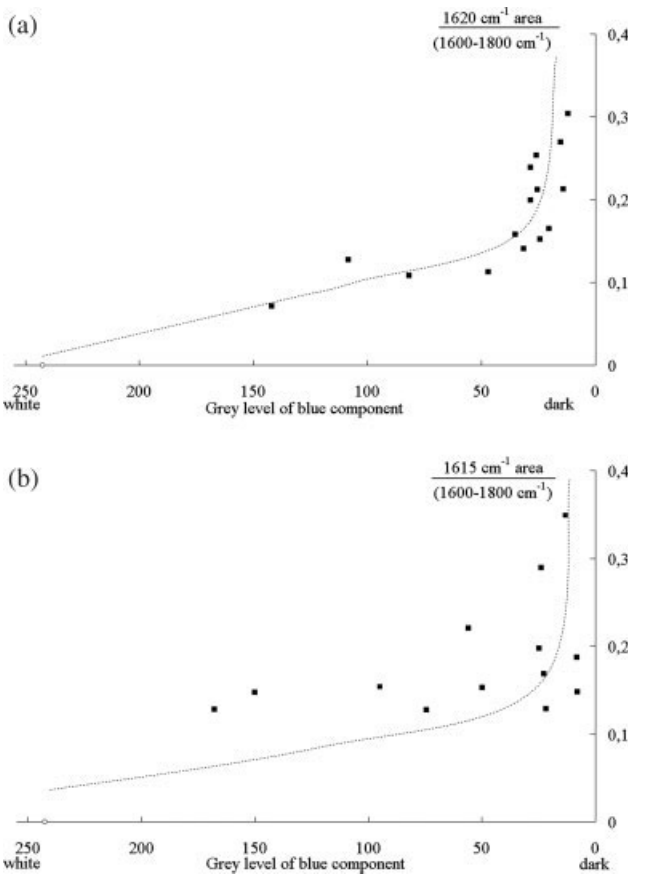

Figure 11 Normalized 1620-cm^{-1} peak area against the level of color of the corresponding (○) pure LDPE and (■) degraded particles: (a) LDPE 1003FE23 and (b) LDPE Lupolen 3721C.

To check if such enol functions can explain degradation color, we have plotted the surface of the most characteristic peak of β-conjugated ketoenol, that is, at 1620 cm^{-1}, normalized by the total area from 1600 to 1800 cm^{-1} against the mean gray level of the blue component of particles for both LDPEs. One can clearly see that the higher 1620-cm^{-1} peak area is, the darker the degraded particles are (Fig. 11). In comparison, the acid function peak area at 1715 cm^{-1}, also normalized, has been plotted against the mean blue level of particles and does not present any correla-

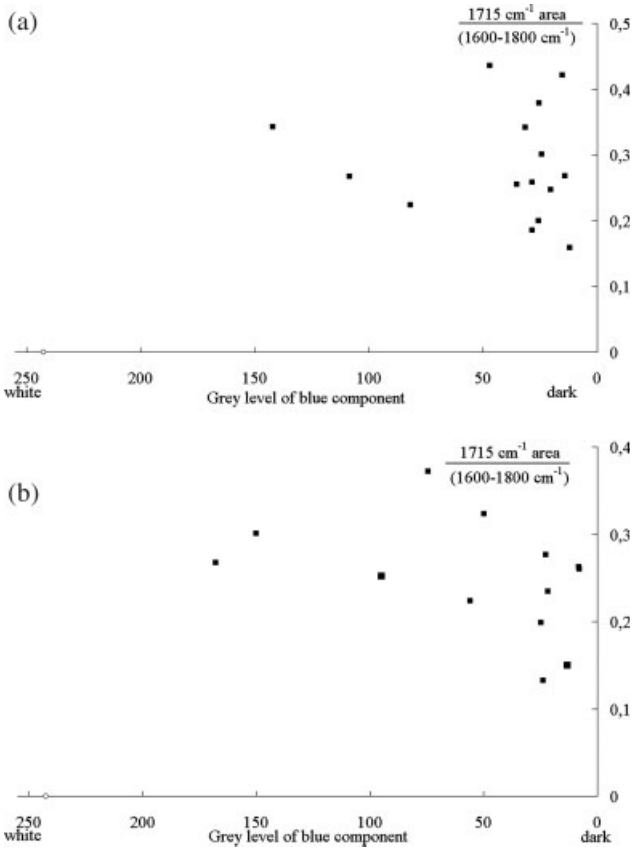

Figure 12 Normalized 1715-cm^{-1} peak area against the level of color of the corresponding (○) pure LDPE and (■) degraded particles: (a) LDPE 1003FE23 and (b) LDPE Lupolen 3721C.

tion with color (Fig. 12). Consequently, the results strongly suggest that such enol functions are responsible for coloration in polyethylene resins.

It would be interesting to observe UV–vis absorption spectra of the degraded particles, but very few experimental techniques have been developed for heterogeneous samples. We thus propose a way to roughly estimate the absorption spectra of particles. It simply consists of analyzing the red, green, and blue mean values of scanned particles (RGB values). Indeed, the sensibility of RGB captors in visible light is Gaussian and centered on a well-defined wavelength corresponding to red, green, and blue, respectively. As a result, RGB values represent in three chromatic points a transmitted beam spectrum after it goes through a particle. Such a spectrum is almost complementary to a particle absorption spectrum. Numerous RGB values of particles of different colors have been analyzed; Figure 13 shows some of them. Reddish particles have a lower blue value and an upper red value, and this means that reddish particles absorb blue light and transmit red color. Dark particles have RGB values that are lower and at nearly the same level, and this means that they have higher absorption.

Quantum simulation

The experimental results in the last section enable us to highlight that particles present IR absorption at 1620 and 1768 cm^{-1} and absorption in blue wavelengths. Indeed, in the past, no relationship has been pointed out between absorption in the visible light domain and the enol structure assumed to be responsible for it. To provide evidence for this last point, quantum calculations were carried out to provide some information about IR and UV–vis absorption spectra of enol functions. The CAChe software was used with the semiempirical method PM5. Three hydrocarbon molecules containing one, two, or three conjugated β-ketoenol functions were created, with 15 carbons for the backbone (Fig. 14). Fifteen carbons were chosen to limit times of calculation and were sufficient for simulations of both electronic and vibration spectra, with aliphatic functions on both extremities of the molecule to be consistent with the polymer structure.

The UV–vis spectrum exhibits an absorption band at 400 nm (violet absorption), which explains the red color of the oxidized particles and confirms the discrete spectra obtained with RGB analysis (Fig. 15). The intensity of this band increases strongly with the conjugation of ketoenol groups and is more and

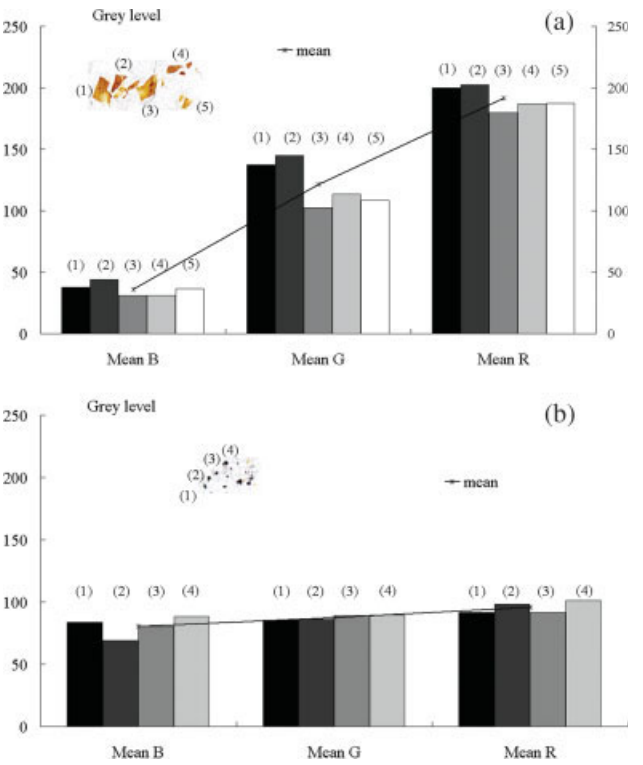

Figure 13 RGB components of degraded particles with different colors: (a) reddish and (b) dark LDPE 1003FE23 extruded under air at L/D = 14.3, 8 rpm, and 135 bars. [Color figure can be viewed in the online issue, which is available at www.interscience.wiley.com.]

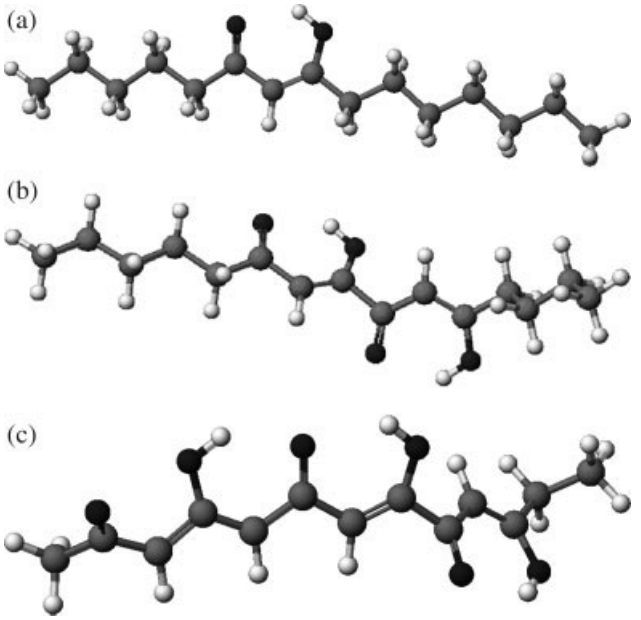

Figure 14 Scheme of simulated molecules with different numbers of conjugated β-ketoenol functions: (a) one, (b) two, and (c) three. The color convention was as follows: oxygen, black; hydrogen, white; and carbon, gray.

more shifted to higher wavelengths, that is, shifted in the visible optical range. Therefore, the more highly conjugated the β ketoenol groups are, the more the material is colored from red to dark, and this shows that the simulated absorption spectra are really connected to the experimental data.

The IR spectra have also been calculated and correspond precisely to the two bands at 1620 and 1768 cm^{-1} of the experimental data (Fig. 16). Their intensity also increases with the number of conjugated enol functions but does not shift in agreement with IR experiments.

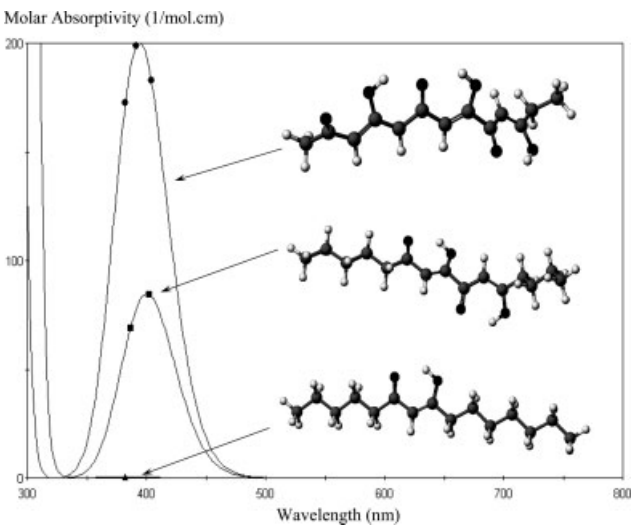

Figure 15 UV–vis spectra of molecules with (●) one, (■) two, and (▲) three conjugated β-ketoenol functions.

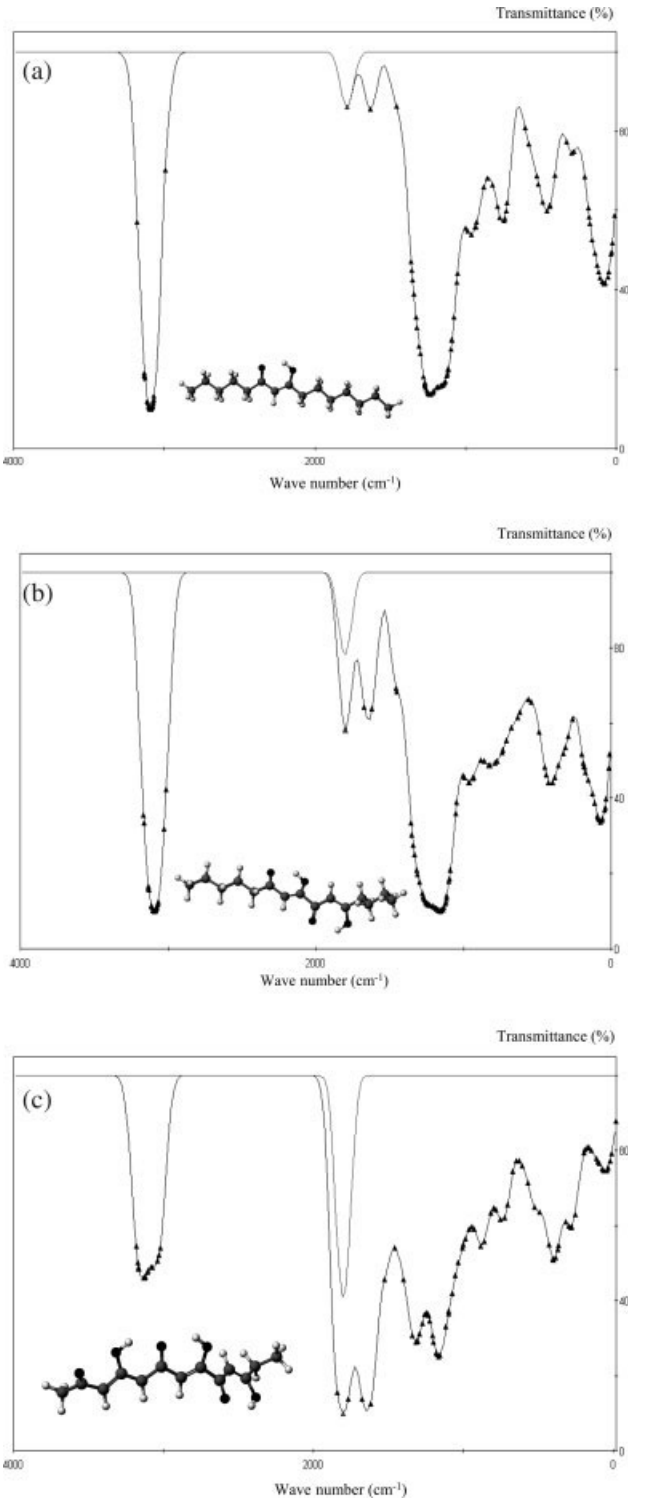

Figure 16 IR spectra of molecules with (a) one, (b) two, and (c) three conjugated β-ketoenol functions.

As a result, the simulation of UV–vis and IR absorption spectra of conjugated β-ketoenol functions confirms the results of Figure 12, which reveals the link between the color of the particles and their specific IR absorption at 1620 and 1768 cm^{-1}.

Discussion of the degradation mechanism

Many kinetic models of polymer melt degradation in processes have been developed.[2,11,18] A global degradation mechanism for thermooxidative degradation is proposed in this part according to the presented results and is compared to those in the scientific literature [eqs. (3) to (9)]. We have seen that under these conditions thermooxidative degradation is favored in comparison with thermomechanical degradation for LDPE extrusion at 270°C. At a high temperature, it is generally agreed that the initiation step in thermooxidation consists of carbon chain scission to form R• radicals [eq. (3)], and this is followed by the formation of $RO_2^•$ radicals in the oxidation step [eq. (4)]:

$$\sim CHR\sim \xrightarrow{h\nu} \sim {}^{\bullet}CHR + R^{\bullet} \quad (3)$$

$$\sim {}^{\bullet}CHR + O_2 \rightarrow \sim RHC-OO^{\bullet} \quad (4)$$

Then, it classically leads to hydroperoxides or peroxides that are very reactive:[2,11]

$$\sim RHC-OO^{\bullet} + \sim CHR'\sim \xrightarrow{10.5\,kcal/mol} \sim RHC-OOH + \sim {}^{\bullet}CR'\sim \quad (5)$$

However, Holmström and Sörvik[10] considered other possible reactions of $RO_2^•$ radicals that are reorganizations of the macrostructure. The first reaction [eq. (7)] is the hydrogenation of $RO_2^•$ by the transfer of the electron to the α-carbon:

$$\sim RHC-OO^{\bullet} = R'-CH_2-CH_2-CHR-OO^{\bullet} \quad (6)$$

$$R'-CH_2-CH_2-CHR-OO^{\bullet} \xrightarrow{37\,kcal/mol} R'-CH_2-CH_2-{}^{\bullet}CR-OOH \quad (7)$$

However, it is a high-energy reaction of 37 kcal/mol that cannot be in competition with the classical reaction [eq. (5)]. The second possible reaction [eq. (8)] is a cyclic reaction of four nodals that transfer an alcohol function to the β-carbon. Because of its low activation energy (11 kcal/mol), it can be as probable as reaction (1)[10] and finally gives an alkene bond:

$$R'-CH_2-CH_2-CHR-OO^{\bullet} \xrightarrow{11\,kcal/mol} R'-CH_2-\underset{\displaystyle HO-O}{CH_2}-{}^{\bullet}CR \rightarrow R'-CH=CH_2-RC-O^{\bullet}+H_2O \quad (8)$$

Then, it may react with another alkyl chain to give β-ketoenol functions, which have been observed by IR microscopy:

$$R'-CH=CH_2-RC-O^{\bullet}+RH \rightarrow R'-CH=CH_2-RC=O+R^{\bullet} \quad (9)$$

However, to have visible degradation as we have observed after 8 h of extrusion, a high concentration of conjugated β-ketoenol functions is necessary (>3, as noticed by quantum simulation). Therefore, a high concentration of oxygen is needed first. Besides, an accumulation of solubilized oxygen in oxidized sites on macromolecular chains is energetically favored because of van der Waals attractions. Thus, the high solubility of oxygen in oxidized areas should contribute to the preferential growth of already degraded volumes. That can explain why degradation is heterogeneous and observed in the particle form.

Second, a high concentration of chemical functions is needed. Again, the formation of numerous conjugated β-ketoenol functions is energetically favored. We think that the first β-ketoenol function is formed by the global degradation mechanism as explained previously. Then, a second carbonyl function may be produced on the β-carbon that finally produces a second conjugated β-ketoenol via a tautomeric equilibrium and so on. Indeed, enol tautomeric functions are more stable than the other standard oxidized functions such as saturated aliphatic aldehydes and esters. Such functions are observed in IR spectra of degraded particles and may be caused by the propagative reaction [eq. (5)], which is also as probable as reaction (8), which leads to conjugated β ketoenol. Taatjs et al.[19] also observed that hydrocarbon oxidation induced the formation of two, three, and four carbon enols, but without the correlating color of degradation in the presence of such functions. It is the very first time that a link between the presence and formation of conjugated β ketoenol and the color of degradation has been established.

CONCLUSIONS

We have studied degradation at a high processing temperature during LDPE extrusion. Dark dots coming from degradation appear in the process, especially in the region in which melt flow has stagnated.

We report important practical and theoretical results:

- Inert gases (nitrogen and carbon dioxide) are highly effective in eliminating degradation particles and are much more effective than an antioxidant. The influence of pressure inside the process on degradation seems to be connected to gas solubility in the polymer melts, but the main effect is gas convection by the polymer. Indeed,

there is no significant difference between the two inerting gases. Besides, no connection between the screw speed or shear rate with degradation has been established, and this proves the nature of degradation to be essentially thermooxidative and not mechanical.

- Chromophore groups, that is, conjugated β ketoenols, have been discovered to be responsible for the color of degradation, and this has been confirmed by quantum simulations.

The experiments have been performed with LDPE resins, but the results may also be applicable to other polyolefins. Further investigations are still required to thoroughly understand the development of enol functions.

References

1. Ramès-Langlade, G.; Monasse, B.; Milési, M. Caoutchoucs Plast 2005, 830, 34.
2. El'darov, E. G.; Mamedov, F. V.; Gol'dberg, V. M.; Zaikov, G. E. Polym Degrad Stab 1996, 51, 271.
3. Kometani, H.; Matsumura, T.; Suga, T.; Kanai, T. Yamagata 2006, 22, G01–18.
4. Andersson, T.; Stalbom, B.; Wesslen, B. J Appl Polym Sci 2004, 91, 1525.
5. Dalbey, W. E.; Byrum, L. M.; Mooney, J. K.; Pulkoswski, C. H.; Herry, L. D. Annu Tech Conf 1992, 92, 202.
6. Barabas, K.; Irving, M.; Kelen, T.; Turos, F. J Appl Polym Sci Polym Symp 1976, 57, 65.
7. Hoff, A.; Jacobsson, S. J Appl Polym Sci 1981, 26, 3409.
8. Rideal, G. R.; Padget, J. C. J Polym Sci Polym Symp 1976, 57, 1.
9. Holmström, A.; Sörvik, E. J Appl Polym Sci 1974, 18, 761.
10. Holmström, A.; Sörvik, E. J Appl Polym Sci 1974, 18, 779.
11. King, R. E., III. J Plast Film Sheeting 2002, 18, 179.
12. Ballenger, T. F.; White, J. L. J Appl Polym Sci 1971, 15, 1949.
13. Dubrocq, C.; Monasse, B.; Milesi, M.; Ramès-Langlade, G. Yamagata 2006, 22, G01-19.
14. Newitt, D. M.; Weale, K. E. J Chem Soc 1948, 1541.
15. Flaconnèche, B.; Martin, J.; Klopffer, M. H. Oil Gas Sci Technol Rev IFP 2001, 56, 261.
16. Hoff, A.; Jacobsson, S.; Pfaffli, P.; Zitting, A.; Frostling, H. Scand J Work Environ Health 1982, 8, 1.
17. Sato, Y.; Fujiwara, K.; Sumarno, T. T.; Takishima, S.; Masuoka, H. Fluid Phase Equilib 1999, 162, 261.
18. Epacher, E.; Tolveth, J.; Stoll, K.; Pukansky, B. J Appl Polym Sci 1999, 74, 1596.
19. Taatjs, C. A.; Hansen, N.; Mcllroy, A.; Miller, J. A.; Senosiain, J. P.; Klippenstein, S. J.; Qi, F.; Sheng, L.; Zhang, Y.; Cool, T. A.; Wang, J.; Westmoreland, P. R.; Law, M. E.; Kasper, T.; Kohse-Höinghaus, K. Science 2005, 308, 1887.
20. Bravo, A.; Hotchkiss, J. M. J Appl Polym Sci 1993, 47, 1741.